

# Virtual Reference Feedback Tuning with robustness restrictions: a swarm intelligence solution

Luan Vinícius Fiorio<sup>a,b,\*</sup>, Chrystian Lenon Remes<sup>c,d</sup>, Yales Rômulo de Novaes<sup>b</sup>

<sup>a</sup>*Department of Electrical Engineering, Eindhoven University of Technology, Eindhoven, 5600 MB, Noord-Brabant, the Netherlands*

<sup>b</sup>*Department of Electrical Engineering, Santa Catarina State University, R. Paulo Malschitzki, 200 - Zona Industrial Norte, Joinville, 89219-710, Santa Catarina, Brazil*

<sup>c</sup>*Department of Electrical Engineering, Federal University of Paraná, Rua XV de Novembro, 1299, Curitiba, 80060-000, Paraná, Brazil*

<sup>d</sup>*Department of Electrical Engineering, Federal University of Rio Grande do Sul, V. Osvaldo Aranha, 103 - Centro Histórico, Porto Alegre, 90035-190, Rio Grande do Sul, Brazil*

---

## Abstract

This work proposes the inclusion of an  $\mathcal{H}_\infty$  robustness constraint to the Virtual Reference Feedback Tuning (VRFT) cost function, which is solved by metaheuristic optimization with only a single batch of data (one-shot). The  $\mathcal{H}_\infty$  norm of the sensitivity transfer function is estimated in a data-driven fashion, based on the regularized estimation of the system's impulse response. Four different swarm intelligence algorithms are chosen to be evaluated and compared at the optimization problem. Two real-world inspired examples are used to illustrate the proposed method through a Monte Carlo experiment with 50 runs. To compare the swarm intelligence algorithms to each other, 50 search agents have been adopted, with a maximum number of iterations of 100.

*Keywords:* Data-driven control, Robust control, Swarm intelligence algorithms, Virtual Reference Feedback Tuning

---

\*Corresponding author.

*Email addresses:* [l.v.fiorio@tue.nl](mailto:l.v.fiorio@tue.nl) (Luan Vinícius Fiorio), [chrystian.remes@ufrgs.br](mailto:chrystian.remes@ufrgs.br) (Chrystian Lenon Remes), [yales.novaes@udesc.br](mailto:yales.novaes@udesc.br) (Yales Rômulo de Novaes)

## 1. Introduction

In several processes of different nature, the inherent complexity to obtain a detailed model sometimes require the designer to simplify the modeling in order to be able to control the plant [1]. In some cases, as for power systems [2, 3], a precise model of the grid is required to design a satisfactory controller. For dc-dc converters, for example, the majority of the control techniques assume the existence of an accurate model [4, 5], presenting a challenge to the designer since power converters have nonlinear dynamics. Another situation that presents difficulty to the designer is the obtention of robust low order controllers, such as PI and PID controllers, which are simpler to be implemented and are vastly applied in industry [6, 7, 8, 9]. This can be originated from a poor modeling due to the process complexity, and/or from the limited performance of the chosen controller structure [10].

In another hand, data-driven control design techniques are used to overcome common problems related to models, such as the dilemma on representativity and complexity, or even unavailability of them [11, 12, 13]. Some of the data-driven approaches require several plant experiments and iterative acquisition of data, as Iterative Feedback Tuning (IFT) [14] and Correlation-based Tuning (CbT) [15], whilst others as Virtual Reference Feedback Tuning (VRFT) [16], Direct Iterative Tuning (DIT) [17], Optimal Controller Identification (OCI) [18], Virtual Disturbance Feedback Tuning (VDFT) [19], and Data-Driven Linear Quadratic Regulator (DD-LQR) [20] only require a single batch of data in order to tune the controller parameters. Having a one-shot method can be a desirable feature in data-driven control design because it requires simpler experimentation, less memory requirements, and results in a less tedious process.

Robustness considering low order controllers is a frequent topic of discussion [21, 22], since certain processes can present uncertainties, as well as disturbances that might occur over time. Another point to be observed is that a poor choice of reference model or limited controller class in, e.g., the VRFT design, may result in poor performance or robustness [23]. Since robustness can be measured by the  $\mathcal{H}_\infty$  norm of the sensitivity transfer function  $S(z)$  of a closed-loop system [24], its inclusion to the data-driven design of controllers could be considered, allowing for a more robust design when necessary. A recent methodology proposed in [25] has suggested the inclusion of robustness criteria in the VRFT design, at the expense of: i) more experiments, since the proposed design procedure iterates in a trial-and-error

fashion until the desired robustness is achieved, and essentially removes one of the greatest advantages of the VRFT - being a one-shot method; and ii) this type of iterative procedure usually requires more background knowledge from the designer for choosing reference models and specifying requirements. A recent data-driven one-shot approach for multivariable systems regarding robust solutions of  $\mathcal{H}_2$ ,  $\mathcal{H}_\infty$  criteria, and loop-shaping specifications, has been recently addressed [26], which relies on an initial solution that influence the final one since it is convexified by linearization around the initial stabilizing controller. In the case of data-driven one-shot approach for SISO systems, considering an  $\mathcal{H}_\infty$  robust performance criteria, a recent work [27] presents a solution that increase the controller order as the solution converges, only dealing with noise-free data. Both methods [26, 27] use only frequency-domain data. Other data-driven robust solutions are achieved in an online fashion and require higher computational processing than offline techniques, and also have the need to measure signals in real-time. Some of those techniques are the use of the modified Riccati equation with online data-driven learning [28] and the application of a data-driven Model Predictive Control method with robustness guarantees [29].

Among the aforementioned data-driven design techniques, the VRFT has been more broadly applied to a several class of problems, fact that can be useful to attest the feasibility of the proposed method of this paper, as well as it requires less computational cost than, e.g., OCI and online methods. Therefore, this work is based on the VRFT technique, as presented in [16] and [30], proposing the inclusion of the  $\|S(z)\|_\infty$  norm criteria in the VRFT design maintaining one of its most attractive features, which is the necessity of a single batch of data. In order to achieve such robustness requirements, the robustness criteria is inserted as a constraint in the VRFT optimization problem, in the form of a penalty [31], which compromises the convex behavior of the VRFT cost function. To deal with this non-convex optimization procedure, the proposed method is tackled in two main steps: i) design, in a data-driven fashion, a controller using the VRFT approach, if a previous controller is unexistent; and ii) considering the controller from the previous step as initial solution and using the same batch of data, apply a metaheuristic optimization algorithm to minimize the cost function considering an  $\|S(z)\|_\infty$  norm constraint.

Since metaheuristic algorithms may do well for a class of problems, but worse over other class of problems, according to the No Free Lunch (NFL) theorems [32], more than a single metaheuristic optimization algorithm must

be evaluated. Looking over the available types of metaheuristics, three can be highlighted: evolutionary algorithms [33]; physics-based algorithms [34]; and swarm intelligence algorithms. Although some authors group evolutionary algorithms with multiple agents and swarm algorithms together [35], this paper considers the two classes separately, as done by other authors in the metaheuristic optimization subject [36]. This work focus on swarm intelligence algorithms, since they have usually less parameters to be tuned by the user or designer [35]. Four swarm intelligence algorithms are considered: Particle Swarm Optimization (PSO) [37] and Artificial Bee Colony (ABC) [38], since those are two of the most used in literature; and the two swarm intelligence algorithms with the least number of hyperparameters, Grey Wolf Optimizer (GWO) [36], and its most recent version, the Improved Grey Wolf Optimizer (I-GWO) [39].

This paper is structured as follows: Section 2 describes the system that is considered in this paper for the theoretical formulation; Section 3 presents the basis of data-driven controller design and details the basic VRFT design procedure; Section 4 explains the method for  $\mathcal{H}_\infty$  norm estimation of the sensitivity transfer function; Section 5 details the four used swarm intelligence algorithms; Section 6 presents the proposed method; Section 7 illustrates and validates the method by showing its application in two real-world inspired examples; and finally, Section 8 concludes this work.

## 2. Preliminaries: description of the system

The system considered in this paper for the theoretical formulation is a discrete-time, causal, linear time-invariant, and Single-Input Single-Output (SISO) system  $G(z)$ . It is considered that  $z$  is the forward discrete time-shift operator such that  $zx(k) = x(k+1)$ . The output  $y(k)$  of this system can be described as

$$y(k) = G(z)u(k) + v(k), \quad (1)$$

where  $u(k)$  is the input signal and  $v(k)$  is the process noise - stochastic effects that are not represented by  $G(z)$ , i.e., not captured by the input-output relation of  $u(k)$  and  $y(k)$ .

The closed-loop system taken into account in this work regards a controller  $C(z)$  with the process  $G(z)$  and a unit gain feedback, as shown in Figure 2, where  $r(k)$  is the reference signal and  $e(k)$  is the error signal. The

closed-loop control law is

$$u(k) = C(z, \rho)(r(k) - y(k)), \quad (2)$$

with

$$C(z, \rho) = \rho' \bar{C}(z) \quad (3)$$

being a controller with parameter  $\rho \in \mathbb{R}^p$ ,  $\bar{C}(z)$  a vector of transfer functions belonging to the controller class  $\mathcal{C}$  (e.g., PI or PID controller classes) and  $r(k)$  the reference signal.

The output of the closed-loop system is given as

$$y(k) = T(z)r(k) + S(z)v(k), \quad (4)$$

where the reference signal  $r(k)$  is applied to the transfer function from the reference  $r(k)$  to the output  $y(k)$ ,  $T(z)$ , with

$$T(z) = \frac{C(z)G(z)}{1 + C(z)G(z)}, \quad (5)$$

and  $S(z)$  is the sensitivity transfer function such that  $S(z) + T(z) = 1$  and

$$S(z) = \frac{1}{1 + C(z)G(z)}. \quad (6)$$

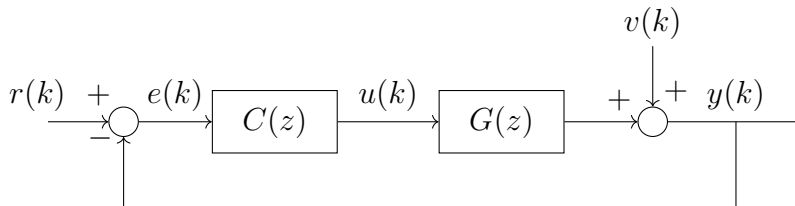


Figure 1: Block diagram of the considered closed-loop system structure for this paper.

In the next section, the Model Reference Control (MRC), which is the basis for the VRFT, is introduced. The VRFT method is described for the cases where the process has a minimum and non-minimum phase.

### 3. Data-driven controller design

The Model Reference Control (MRC), which is the basis for the VRFT, more generally called as model matching control [40], concerns reference tracking of the closed-loop system's response to the reference, disregarding the effects of noise at the output [23].

In order to obtain a controller, the MRC requires the designer to elaborate a target transfer function for the controlled closed-loop system, called reference model ( $T_d(z)$ ), which generates the output  $y_d(k) = T_d(z)r(k)$ . A reference tracking performance criterion evaluated by the two-norm tracking error is then obtained by solving the optimization problem

$$\underset{\rho}{\text{minimize}} \quad J^{MR}(\rho) = \|(T(z, \rho) - T_d(z))r(k)\|_2^2 \quad (7)$$

which can be solved considering (5), resulting in the solution controller for the MRC, which is called ideal controller  $C_d(z)$ .

#### 3.1. Virtual Reference Feedback Tuning

The VRFT is a one-shot optimization data-driven controller design technique based on the MRC. It is defined as one-shot since only a single batch of input-output data is required to solve the model reference control problem (7), which can be done by the use of least squares when the controller is linearly parametrized as in (3), resulting in the parameter  $\rho$  of a controller with predefined class. The VRFT design depicted in this paper follows the procedures of [23, 11].

Consider an experiment, in open-loop or closed-loop, that results in a batch of collected data  $\{u, y\}_{k=1}^N$ . A *virtual reference* signal  $\bar{r}(k)$  is defined such that  $T_d(z)\bar{r}(k) = y(k)$ . A virtual error can be obtained as  $\bar{e}(k) = \bar{r}(k) - y(k) = (T_d^{-1}(z) - 1)y(k)$ . In summary, a controller  $C(z, \rho) = \rho' \bar{C}(z)$  is considered satisfactory if it generates  $u(k)$  when fed by  $\bar{e}(k)$ . The closed-loop block diagram for the VRFT controller design is illustrated in Figure 2.

The VRFT solves the optimization problem

$$\underset{\rho}{\text{minimize}} \quad J^{VR}(\rho) = \|u(k) - C(z, \rho)(T_d^{-1}(z) - 1)y(k)\|_2^2 \quad (8)$$

which has the same minimum as (7) if the ideal controller  $C_d(z)$  in (5) belongs to the same controller class  $\mathcal{C} = \{C(z, \rho), \rho \in \mathbb{R}^p\}$  as  $C(z, \rho)$ . To compensate the fact that the ideal controller rarely belongs to the chosen controller class,

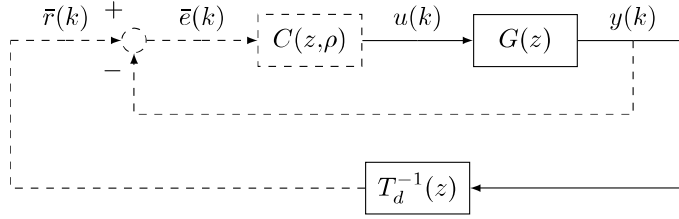


Figure 2: Closed-loop block diagram for the VRFT controller design.

a filter  $L(z)$  is applied to the data to approximate the minimum of  $J^{VR}$  to the minimum of  $J^{MR}$ , which amplitude should satisfy [23]:

$$|L(e^{j\Omega})|^2 = |T_d(e^{j\Omega})|^2 |1 - T_d(e^{j\Omega})|^2 \frac{\Phi_r(e^{j\Omega})}{\Phi_u(e^{j\Omega})}, \quad \forall \Omega \in [-\pi, \pi], \quad (9)$$

where  $x(e^{j\Omega})$ , with  $x$  representing any signal or system, represents the Discrete Fourier Transform of  $x(k)$ ,  $\Phi_r(e^{j\Omega})$ ,  $\Phi_u(e^{j\Omega})$  are, respectively, the power spectra of the signals  $r(k)$ ,  $u(k)$ .

Instrumental variables can be used in order to suppress estimation bias caused by the noise in data [41], requiring the use of a second data batch. In practice, the input signal can be formed by two identical sequences at the same experiment, if memory restrictions do not impose a problem. Then, the signals can be synced together afterwards, resulting in two batches of data from one single experiment.

In the presence of a Non-Minimum Phase (NMP) zero at the process, a flexible reference model can be used, as presented in [23]. The optimization problem (8), then, becomes

$$\underset{\rho}{\text{minimize}} \quad J^{VR}(\rho) = \|\eta' F(z)(u(k) + \rho' \bar{C}(z)y(k)) - \rho' \bar{C}(z)y(k)\|_2^2 \quad (10)$$

where  $\eta \in \mathbb{R}^m$ , and  $F(z)$  is a vector of transfer functions such that  $T_d(z, \eta) = \eta' F(z)$ . The step-by-step design for the VRFT with flexible reference model, from data collection to the algorithm design, is detailed in [11].

To be able to include a robustness criteria at the VRFT cost function, a means of evaluating this parameter is required. Nonetheless, this is approached in the next section.

#### 4. Robustness index estimation

Depending on the choice of  $T_d(z)$  or the controller class  $\mathcal{C}$ , as well as the response of the plant  $G(z)$ , the VRFT-designed controller can result in poor robustness of the controlled process. For such cases, a robustness constraint can be included in the form of the  $\mathcal{H}_\infty$  norm of  $S$ , here called  $M_S$ , which can be used as a measure of robustness [24].

Typically, a system that presents  $M_S > 2$  is considered to have poor robustness [24]. In this context, and considering the use of data-driven design approaches, it is needed to estimate the value of  $\|S(z)\|_\infty$  only using data, since it is assumed that no plant model is available to the designer. From this reasoning, the estimation of  $M_S$  is explained in the following subsection.

##### 4.1. Estimation of $M_S$

The  $\mathcal{H}_\infty$  norm estimation procedure developed in this work is based on the Impulse Response (IR) of the system, as presented in [42], modified from [43] to a SISO impulse response identification procedure, which allows for a regularized estimation according to existing literature [44]. Also, in order to maintain the one-shot characteristic of the VRFT, the estimation of the  $\mathcal{H}_\infty$  norm of  $S$  ( $M_S$ ), based on its impulse response, and considering a single batch of data is addressed as follows: consider the linear discrete-time causal and SISO system  $S$ , represented by its transfer function  $S(z, \rho)$ , such that its output signal  $\psi(k)$  is given by the convolution

$$S : \psi(k) = s(k) * \zeta(k) = \sum_{n=0}^{\infty} s(k-n)\zeta(n), \quad (11)$$

where  $\zeta(k)$  is the input signal of  $S$ , whose impulse response is  $s(k)$ .

Since (11) requires infinite data to be obtained, an order  $M$  is defined such that it is assumed that any IR term greater than  $M$  is negligible, which is valid for stable systems, since  $\lim_{k \rightarrow \infty} s(k) = 0$ . Nevertheless, the convolution in (11) can be truncated to  $M$  terms, leading to:

$$S : \psi(k) = \sum_{n=0}^{\infty} s(k-n)\zeta(n) \approx \underbrace{\sum_{n=0}^M s(k-n)\zeta(n)}_{|s(M+1)| < \epsilon, \text{ with } \epsilon \rightarrow 0^+} . \quad (12)$$



On the other hand, the definition of  $\mathcal{H}_\infty$  norm, when applied to the system  $S$ , can be written as [24]

$$\mathcal{H}_\infty : \|S\|_\infty = \max_{\zeta(k) \neq 0} \frac{\|s(k) * \zeta(k)\|_2}{\|\zeta(k)\|_2}, \quad (13)$$

which requires the whole set of possible inputs  $\{\zeta(k) \neq 0\}$ . Therefore expression (13) cannot be directly calculated. An alternative strategy is to obtain a matrix relation for  $S$ , which allows for the use of induced norm properties. Expanding (12) to the  $M$  first terms,

$$\left\{ \begin{array}{l} \psi(0) = s(0)\zeta(0) \\ \psi(1) = s(1)\zeta(0) + s(0)\zeta(1) \\ \vdots \\ \psi(M) = s(M)\zeta(0) + \dots + s(0)\zeta(M), \end{array} \right. \quad (14)$$

the following matrix relation truncated at  $M$  elements is obtained:

$$\underbrace{\begin{bmatrix} \psi(0) \\ \psi(1) \\ \dots \\ \psi(M) \end{bmatrix}}_{\Psi_M} = \underbrace{\begin{bmatrix} s(0) & 0 & \dots & 0 \\ s(1) & s(0) & \dots & 0 \\ \vdots & \vdots & \ddots & \vdots \\ s(M) & s(M-1) & \dots & s(0) \end{bmatrix}}_{S_M} \underbrace{\begin{bmatrix} \zeta(0) \\ \zeta(1) \\ \dots \\ \zeta(M) \end{bmatrix}}_{Z_M}. \quad (15)$$

From the assumption that the order  $M$  is sufficiently high, it can be said that matrix  $S_M$  characterizes the IR  $s(k)$  of  $S$ .

An useful matrix property is the induced norm [24, A.5], which can be applied to (15), such that:

$$\|S_M\|_{ip} = \max_{Z_M \neq 0} \frac{\|S_M Z_M\|_p}{\|Z_M\|_p}, \quad (16)$$

where the subscript  $i$  stands for induced. In short, (16) is a matrix form of representing the system gain considering a set of possible input signals  $Z_M$ . From the induced-2 norm, it is obtained that

$$\|S_M\|_{i2} = \bar{\sigma}(S_M) = \sqrt{\lambda_{max}(S'_M S_M)}, \quad (17)$$

where  $\bar{\sigma}$  and  $\lambda_{max}$  stands for largest singular value and largest eigenvalue, respectively, and comparing (13) with (16), it can be seen that

$$\|S\|_{\infty} \approx \max_{Z_M \neq 0} \frac{\|S_M Z_M\|_2}{\|Z_M\|_2} = \sqrt{\lambda_{\max}(S'_M S_M)}. \quad (18)$$

Since the  $\|S(z, \rho)\|_{\infty}$  norm can be estimated based on its IR via (18), an expression for the input signal  $\zeta(k)$  and the output signal  $\psi(k)$  of  $S(z, \rho)$  shall be obtained in order to estimate its impulse response in the VRFT design context.

#### 4.1.1. Input-output signals of the sensitivity transfer function

Considering the system presented in Figure 2, its sensitivity transfer function in (6) can be rewritten as

$$1 + C(z, \rho)G(z) = S^{-1}(z, \rho). \quad (19)$$

Assuming that  $u(k)$  is sufficiently informative to capture all relevant characteristics of  $S(z, \rho)$ , and multiplying both sides of (19) by  $u(k)$ , it is obtained that

$$u(k) + C(z, \rho)G(z)u(k) = S^{-1}(z, \rho)u(k). \quad (20)$$

It is known that  $G(z)u(k) = y(k)$ . Substituting such relation in (20):

$$u(k) + C(z, \rho)y(k) = S^{-1}(z, \rho)u(k). \quad (21)$$

Finally, the signals

$$\xi(k) = u(k), \quad \zeta(k) = u(k) + C(z, \rho)y(k), \quad (22)$$

can be defined, which means that when a signal  $\zeta(k)$  formed by  $u(k) + C(z, \rho)y(k)$  is applied to  $S(z, \rho)$ , an output  $\xi(k) = u(k)$  is obtained. Therefore, the impulse response of  $S(z, \rho)$  can be estimated considering the data set  $\{\xi, \zeta\}_{k=1}^N$ , as presented in (22).

In this work, the IR estimation is done through identification with regularization techniques, since: i) the variance of the estimates increases with  $M$ , which is suppressed with the use of regularization [44]; and ii) knowing that IR is a sparse signal for sufficiently high  $M$ , the use of regularization is known to improve sparse signal estimates [45]. The algorithm for regularized estimation of impulse response is described in [44, 46], and it is available in MATLAB® [47], Python [48], and R [49].

The inclusion of an  $\|S(z, \rho)\|_\infty$  constraint in the problem (VRFT cost function (8)) to be minimized spoils the convexity characteristic of the VRFT method and the solution cannot be obtained anymore through the least squares algorithm. A strategy to deal with local minima and other characteristics that may arise from a non-convex cost function is to use metaheuristic optimization [50]. Nevertheless, this work addresses the use of swarm intelligence algorithms to solve the proposed problem, which are described in the following section.

## 5. Swarm intelligence algorithms

Swarm intelligence algorithms consist of algorithms that are based on the collective intelligence of groups composed by simple agents, usually based on the behavior of animals in nature [51]. In order to cope with the NFL theorems [32], four algorithms are chosen to be used:

1. Particle Swarm Optimization (PSO) [37];
2. Artificial Bee Colony (ABC) [52];
3. Grey Wolf Optimizer (GWO) [36];
4. Improved Grey Wolf Optimizer (I-GWO) [39].

The PSO and ABC algorithms are well known and widely used in metaheuristic optimization regarding swarm intelligence algorithms [50, 53]. The GWO algorithm is more recent and presented some interesting results, as well as it has less hyperparameters than the aforementioned, which is a desirable feature. At last, the I-GWO algorithm is the most recent, which improves the GWO aiming to avoid local minima. The four algorithms are briefly commented in the subsections below.

### 5.1. Particle Swarm Optimization

Particle swarm optimization is a stochastic optimization technique that mimics the social behavior of flocking, schooling, and buzzing of animals like birds, fish, and bees. It involves populations (or swarms) in which each element is called a *particle*. Each particle follows a social behavior under the swarm, representing a form of directed mutation, which maintains a static population number during the whole optimization procedure [53, 37].

The swarm is composed by  $\ell$  particles searching in a  $D$ -dimensional space, which are initialized randomly within the search space. Each particle has its own position ( $\vec{X}_i$ ) and velocity ( $\vec{V}_i$ ) and is considered as a possible solution

for the problem. The best solution ever found locally by a particle  $i$  is represented by  $\vec{P}_i = \{P_{i1}, P_{i2}, \dots, P_{iD}\}$ , while  $\vec{G} = \{G_1, G_2, \dots, G_D\}$  is the best solution found by the whole swarm, i.e., globally. As for the standard algorithm, each particle starts at a random location with random velocity.

Each new value of position and velocity of a particle depends on its previous value and its neighbourhood. At each iteration, velocity is updated as

$$\vec{V}_i(n) = w_1 \vec{V}_i(n-1) + w_2 C_1 (\vec{P}_i - \vec{X}_i(n-1)) + w_3 C_2 (\vec{G} - \vec{X}_i(n-1)), \quad (23)$$

where  $w_1$  is an inertia weight,  $w_2$  and  $w_3$  are random variables such that  $w_2, w_3 \sim U(0, 1)$ . The constant  $C_1$  is the cognitive learning factor, whilst  $C_2$  is the social learning factor.

After the velocity is updated, the algorithm updates the position of each particle according to

$$\vec{X}_i(n) = \vec{X}_i(n-1) + \vec{V}_i(n). \quad (24)$$

The global solution at the stopping iteration is considered to be the solution of the optimization problem.

## 5.2. Artificial Bee Colony

The artificial bee colony algorithm simulates the behavior of bees performed during their foraging process, conducting local search in each iteration. Possible solutions are represented by food sources, whilst the quality of each solution is proportional to the nectar amount in each source [50, 52].

There are three types of bees: scout, employed, and onlooker. At the initialization, the scout bees find, randomly, possible food sources (solutions). Each food source receive an employed bee. By roulette wheel selection, onlooker bees choose food sources to be exploited based on its quality, but both types perform local search in its neighbourhood.

During the execution of the algorithm, the four phases that occurs at each iteration can be detailed as follows:

1. Initialization phase: the  $\ell$  food sources  $\vec{X}_i = \{X_{i1}, X_{i2}, \dots, X_{iD}\}$  with dimension  $D$ , where  $i = 1, \dots, \ell$ , are initialized randomly
2. Employed bees phase: employed bees search for new food sources having more nectar within its neighbourhood, defined as  $\vec{X}_i(n+1) = \vec{X}_i(n) + r_a(\vec{X}_i(n) - \vec{X}_r(n))$ , where  $\vec{X}_i(n+1)$  and  $\vec{X}_i(n)$  is the food

source at iteration  $n+1$  and  $n$ , respectively,  $r_a$  is a random number such that  $r_a \sim U(-a, a)$  where  $a$  is the acceleration coefficient, and  $\vec{X}_r(n)$  is a randomly selected food source at iteration  $n$ . A greedy selection is applied to the fitness of each food source. The information is then shared with onlooker bees, which are waiting in the hive;

3. Onlooker bees phase: since the onlooker bees receive the information of the food sources from the employed bees, they select randomly a food source  $i$ . After an onlooker bee has chosen a food source, a greedy selection is applied between two sources in the neighbourhood. When there are no more spare food sources, this phase is ended;
4. Scout bees phase: when an employed bee solution cannot be improved anymore, those bees abandon their food sources and become scouts, choosing randomly a new food source  $\vec{X}_i$  where they will be employed. If a user-defined limit number of maximum food sources  $L$  is surpassed, the employed bees on the sources with less food (greater fitness value) will abandon their current food source and become scouts.

Phases 2, 3, and 4 are repeated until an user defined stopping criteria is met. The food source with more food (less cost) at the stopping iteration is considered to be the best solution for the problem.

### 5.3. Grey Wolf Optimizer

The GWO is an algorithm based on the hunting behavior of grey wolves, which have a strict social dominant hierarchy. The leaders are the alphas, responsible for making decisions. At the second level are the betas, subordinates to the alphas that help in decision-making and other pack activities. The third level wolves are the deltas, representing scouts, sentinels, elders, hunters, and caretakers. The rest of the pack is called omega, which must submit to the higher ranking wolves [39].

Respecting the social behavior of wolves, the fittest solution in an optimization fashion is considered to be the alpha (position vector  $\vec{X}_\alpha$ ), whilst second is the beta (position vector  $\vec{X}_\beta$ ), and third the delta (position vector  $\vec{X}_\delta$ ). The rest are assumed to be omega, with position  $\vec{X}_{\omega,k}$ , where  $k$  represent a specific wolf among the omegas with  $k \in \{1 \dots \ell - 3\}$ , and will follow the mean position of the three best wolves. The wolves encircle the prey, reducing the radius as the algorithm advances.

At iteration  $(n + 1)$ , the three wolves with the lowest (best) fitness are considered the new  $\alpha$ ,  $\beta$ , and  $\delta$ . Notice that the wolves move towards the

average of the three best solutions, since they have an encircling behavior for hunting.

The optimization procedure continues until a user defined stopping criteria is met. The best found solution at the stopping iteration, the position of the alpha  $\vec{X}_\alpha$ , is considered the solution of the minimization procedure.

#### 5.4. Improved Grey Wolf Optimizer

There are three main problems perceived in literature around the GWO algorithm [39]: i) lack of population diversity; ii) imbalance between the exploitation and exploration; iii) premature convergence. The improved grey wolf optimizer changes the search strategy of the GWO algorithm, dividing it into three phases - initializing, movement, selecting and updating - which are described below according to [39].

1. Initializing phase:  $\ell$  wolves are randomly distributed in the search space
2. Movement phase: individual hunting by each wolf is included in the algorithm, apart from the base GWO algorithm, with a strategy named Dimension Learning-based Hunting (DLH). A radius is defined as the Euclidean distance between the current position  $\vec{X}_i(n)$  and the candidate position  $\vec{X}_{i,GWO}(n+1)$ , which is calculated exactly as in the standard GWO.  
Then, multi-neighbours learning is performed resulting in the DLH solution  $\vec{X}_{i,DLH}(n+1) = \vec{X}_i(n) + r_i(\vec{X}_n(n) - \vec{X}_r(n))$ , with  $\vec{X}_n(n)$  being a random neighbour,  $\vec{X}_r(n)$  a random wolf, and  $r_i$  a random vector.
3. Selecting and updating phase: the fitness value of the solutions is compared and selected. If the best fitness value until the current iteration, with solution  $\vec{X}_i(n)$ , is greater than  $f(\vec{X}_i(n+1))$ , the best found solution is updated. Otherwise, it remains the same.

The I-GWO algorithm runs until some user defined stopping criteria is met. The position of the alpha wolf  $\vec{X}_\alpha$  at the iteration that the algorithm stops running is considered to be the best solution of the optimization procedure.

The next section details the proposed method of this work, allowing for the inclusion of a robustness criteria at the VRFT cost function, but still maintaining its one-shot characteristic.

## 6. VRFT with robustness restrictions

The proposed method regards a two-step procedure. The first step follows the design of a controller using the VRFT, as commented in Subsection 3.1. At the second step, the same data of the first step is used, avoiding the need of a second experiment, since the estimation of  $M_S$ , which is represented in this context as  $\hat{M}_S(\rho)$ , as proposed in Subsection 4.1, was developed to avoid the need of new data. In this case, the the cost function  $J^{VR}$  is modified by the addition of a robustness restriction, regarding the value of the  $\|S(z, \rho)\|_\infty$  norm, leading to a new optimization problem:

$$\begin{aligned} & \underset{\rho}{\text{minimize}} && J^{VR}(\rho) \\ & \text{subject to} && \hat{M}_S(\rho) \leq M_{Sd}, \end{aligned} \quad (25)$$

which can be applied directly to the cost function as a penalty [31], resulting in the *Swarm Intelligence* optimization cost function:

$$\underset{\rho}{\text{minimize}} \quad J^{SI}(\rho) = \|u(k) - C(z, \rho)(T_d^{-1}(z) - 1)y(k)\|_2^2 + cH(\rho) \quad (26)$$

where  $c$  is a positive constant, usually with  $c \gg 1$ , and the penalty element regarding the estimated ( $\hat{M}_S(\rho)$ ) and desired ( $M_{Sd}$ )  $\mathcal{H}_\infty$  norm value of  $S(z, \rho)$  can be applied as

$$H(\rho) = \frac{1}{2}(\max[0, \hat{M}_S(\rho) - M_{Sd}])^2. \quad (27)$$

The robustness index  $\hat{M}_S(\rho)$  is estimated at each iteration of the swarm algorithm optimization following the procedure described in Subsection 4.1.

Considering a search space  $\mathcal{O} \in [l_b, u_b]$ ,  $l_b, u_b \in \mathbb{R}$ , in order to accelerate the convergence of the metaheuristic algorithm, the initialization of its agents can inherit the first step solution  $\rho_0 \in \mathbb{R}^p$  as a central point, as expressed in

$$\vec{X}_b(0) = R \cdot \vec{X}(0) + \rho_0, \quad R = \frac{|\max\{l_b, u_b\}|}{2}, \quad (28)$$

with  $R$  being the initial population spawn radius, and  $\vec{X}(0) \in \mathbb{R}^p$  a random position vector such that  $\vec{X}(0) \sim U(0, 1)$ .

An inherent step of the method is to collect input-output data from the process, as suggested in [23, 11]. Remember to take into account system identification theory [41] in order for data to be sufficiently informative. Then, the two proposed design steps can be applied:

1. Use the VRFT to design a controller for the process. Use a flexible reference model if the plant is NMP, as presented in [30]. Check the obtained robustness index, proceed to the second step if it does not satisfy  $\hat{M}_S \leq M_{Sd}$ . Such main step can be divided into the following specific steps:
  - acquire a data set  $\{u, y\}_{k=1}^N$  from the closed-loop system with an initial stabilizing controller;
  - use the data set to design a controller with the VRFT method, as detailed in Subsection 3.1. Controller parameters  $\rho$  are obtained after the minimization procedure of the VRFT method. In the NMP case, parameters for the reference model  $\hat{\eta}$  are also obtained;
  - estimate the robustness index according to the method in Subsection 4.1. If  $\hat{M}_S > M_{Sd}$  proceed to the second step, else, use the VRFT-obtained controller with no further modification.
2. Apply a swarm intelligence algorithm considering the optimization problem described in (26) according to a desired value of  $M_S$ , with restriction applied in the form of a penalty as (27), with initial spawn of agents following the recommendation of (28). The second step can be divided in:
  - implement the VRFT cost function with the penalty as in (27) regarding the desired maximum value of  $M_S$ ;
  - change the initialization procedure of the chosen swarm intelligence algorithm to consider a center spawn  $\rho_0$ , i.e., the VRFT-obtained solution at the first step, and a spawn radius as suggested in (28) to accelerate convergence;
  - run the algorithm and obtain controller parameters that satisfy the robustness restriction.

## 7. Validation results

In order to validate and illustrate the proposed method, two real-world inspired examples are considered. The method is applied as suggested in Section 6 with all four swarm intelligence algorithms commented in Section 5. The results are compared in terms of: i) fitness value obtained for best solution (best fitness); ii)  $\|S(z, \hat{\rho})\|_\infty$  value obtained for best solution; iii) convergence speed. It is worthwhile to mention that the system model is



only used to generate data in simulation. The knowledge of the model is neglected at any stage of the design, maintaining a pure data-driven fashion.

### 7.1. Example 1: a second-order plant

The first system to be considered is

$$G_1(z) = \frac{-0.05(z - 1.4)}{z^2 - 1.7z + 0.7325} \quad (29)$$

with a time step of 1 second, which is similar to the discrete-time model of a Boost/Buck-Boost converter operating in Continuous Conduction Mode (CCM) [54]. The presence of a non-minimum phase zero makes it necessary to use the VRFT method with flexible criterion [23] at the first step of the proposed method.

Assuming that the system model (29) is unknown, there is no previous knowledge about its zero being NMP. In this sense, it is possible to analyze the estimated IR, since the IR of NMP systems initially moves in the opposite direction (downwards) related to the steady-state one [45]. Therefore, a Pseudo-Random Binary Signal (PRBS), which is persistently exciting of high order [41], containing  $N = 2000$  samples is applied to  $G_1(z)$  in simulation, generating an output signal. Additive white gaussian noise with a Signal-to-Noise Ratio (SNR) of 20 dB was added to the system at the output, representing measurement noise. With the input-output dataset, the IR of  $G_1(z)$  can be identified with an IR identification algorithm available in the literature [46, 48, 47, 49], resulting in the signal presented in Figure 3. Clearly, the IR initially goes downwards, indicating the presence of an NMP zero, justifying the VRFT with a flexible reference criterion [23].

#### 7.1.1. Data collection

The data for estimation is obtained in closed-loop with a proportional stabilizing controller [11], since its presence in the system avoids signal divergence. By the small gain theorem [24], a stabilizing controller can be obtained as

$$k_p < \frac{1}{\|G\|_\infty}. \quad (30)$$

Therefore, the stabilizing controller  $k_p$  is chosen as

$$k_p = \frac{0.5}{\|G_1(z)\|_\infty} = 0.8039. \quad (31)$$

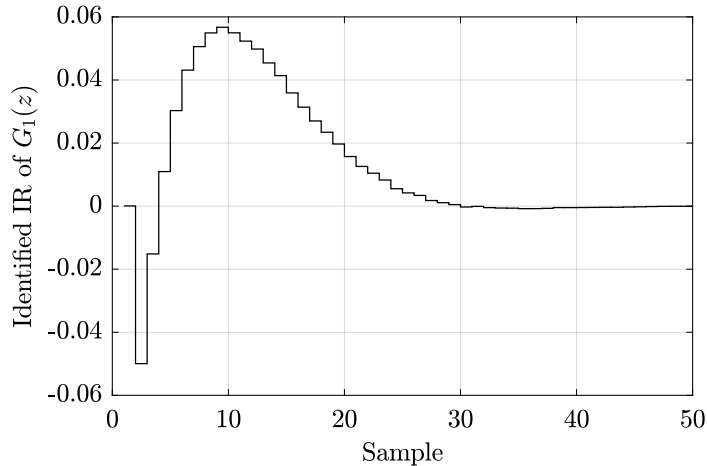


Figure 3: Identified impulse response of  $G_1(z)$ .

In order to obtain the  $\mathcal{H}_\infty$  norm of  $G_1(z)$ , its impulse response is estimated according to [48] and the norm is calculated as proposed in Subsection 4.1.

The input signal considered for the VRFT is a PRBS with  $N = 2000$  samples. It is applied to the control reference of the closed-loop formed by  $G_1(z)$  with stabilizing controller  $k_p$ . The control output signal  $u(k)$  and the system output signal  $y(k)$  are acquired, forming the input-output set  $\{u, y\}_{k=1}^N$ .

#### 7.1.2. Step 1 - VRFT with flexible criterion

Assume a situation where the control requirements are: i) null error in steady-state; ii) settling time approximately 2.5 times faster than in closed-loop with the stabilizing controller  $k_p$ ; iii) null overshoot for a step reference. A reference model, chosen as proposed in [11], that fits the requirements is

$$T_d(z, \hat{\eta}_0) = \frac{-21(z - 1.01)}{(z - 0.7)(z - 0.3)}. \quad (32)$$

Notice that the initial zero of  $T_d(z)$  is set as greater than 1, as suggested in [23], allowing for the VRFT with flexible criterion to identify the plant's NMP zero. The chosen controller class to be used is the PID class of controllers, which gives

$$\bar{C}(z) = \left[ 1 \quad \frac{z}{z-1} \quad \frac{z-1}{z} \right]'. \quad (33)$$

After solving the cost function (10) according to the VRFT method with flexible criterion, the following solution pair of  $\eta, \rho$  is obtained:

$$\hat{\eta} = [-0.4793 \quad 0.6377]' \quad (34a)$$

$$\hat{\rho} = [1.1246 \quad 0.3124 \quad 6.9713]', \quad (34b)$$

resulting in a new reference model  $T_d(z, \hat{\eta})$ , and in the controller  $C(z, \hat{\rho})$ , respectively:

$$T_d(z, \hat{\eta}) = \hat{\eta}F(z) = \frac{-0.6899(z - 1.33)}{(z - 0.7)(z - 0.2401)}, \quad (35a)$$

$$C(z, \hat{\rho}) = \hat{\rho}'\bar{C}(z) = \frac{8.4083(z^2 - 1.792z + 0.8291)}{z(z - 1)}. \quad (35b)$$

The non-dominant pole of the reference model, now  $T(z, \hat{\eta})$ , is updated altogether with the minimization of  $\eta$  and  $\rho$ , as suggested in [11].

By estimating the  $\mathcal{H}_\infty$  norm of  $S(z, \hat{\rho})$  of the closed-loop system based on the solution (35), an  $M_S = 2.1952$  is obtained, which may be too high for applications that require lower robustness indexes, since it is greater than 2 [24]. The next subsection presents the application of the second step of the proposed method to reduce  $M_S$  for the obtained VRFT solution.

### 7.1.3. Step 2 - Swarm intelligence algorithm

Four swarm intelligence algorithms - PSO, ABC, GWO, and I-GWO - were used to solve the problem (26) for an initial solution of  $\rho_0$  (34b), with upper search bound  $u_b = 10$ , which should be sufficient considering that the maximum  $\rho$  value of the VRFT-obtained controller is 6.9713 and, taking into account a choice of  $M_{Sd}$  that is not too ambitious, the parameters values should not differ that much from the initial ones. The lower search bound  $l_b$  is chosen as  $l_b = 0$  to avoid negative controller gain, making the obtained controller passive [55]. The reference model for the swarm intelligence algorithm minimization is considered to be the one obtained through the VRFT with flexible criterion,  $T_d(z, \hat{\eta})$ . Also, an initial population spawn radius of  $R = u_b/2 = 5$  is considered, as suggested in (28). The desired  $M_S$  to be achieved,  $M_{Sd}$ , was set to 1.8, which is a sufficient value in terms of robustness, satisfying  $M_{Sd} \leq 2$ , and also should not compromise substantially the performance of the system.

To make the comparison between algorithms possible, the number of agents was fixed to 50, as well as the number of iterations, limited to 100. In order to obtain a satisfactory number of realizations for the analysis of results each algorithm was run 50 times. The parameter settings that are chosen by the designer for the PSO and ABC algorithms, except from the number of agents and maximum number of iterations, are presented in Table 1. The PSO parameters were chosen as the MATLAB<sup>®</sup> default parameters of the Global Optimization Toolbox [47], whilst the ABC parameters were used according to the algorithm implementation of [56]. GWO and I-GWO do not contain any hyperparameter set by the user aside from number of agents and maximum number of iterations.

Algorithm	Parameter settings	Value
PSO	Cognitive learning factor ( $C_1$ )	1.49
	Social learning factor ( $C_2$ )	1.49
	Inertia range (range of $w_1$ )	[0.1,1.1]
ABC	Limit of food sources ( $L$ )	90
	Acceleration coefficient ( $a$ )	1

Table 1: Parameters settings for PSO and ABC.

Figure 4 shows the average convergence curve of all algorithms for 50 runs, considering system  $G_1(z)$  as aforementioned. Table 2 presents the time that each iteration took and the number of iterations needed to converge, considering the average value for all 50 realizations and a criteria of convergence with a variation of  $\delta = 1 \times 10^{-3}$  from a sample to the subsequent one. The results were obtained with an Intel Core i5 4670 3.40 GHz processor, with 8 GB of RAM - DDR3 1600 MHz. The I-GWO algorithm took a longer time to converge, followed by ABC, PSO, and at last, GWO. Considering all 50 runs, Figure 5 presents the best fitness statistics obtained for all algorithms in the form of a box plot. Clearly, I-GWO had the most desired performance in terms of fitness, since it contains less outliers and a very low dispersion if compared to the other algorithms' solutions. PSO, ABC and GWO, in general, resulted in higher fitness values than I-GWO for the considered cost function. Table 3 shows the quantitative values related to the best fitness of all algorithms at each run, confirming the conclusions taken from Figure 5.

Finally, Figure 6 presents the box plot for the obtained  $\|S(z, \hat{\rho})\|_\infty$  by the best solution of each algorithm at each run, in a closed-loop with  $G_1(z)$ .

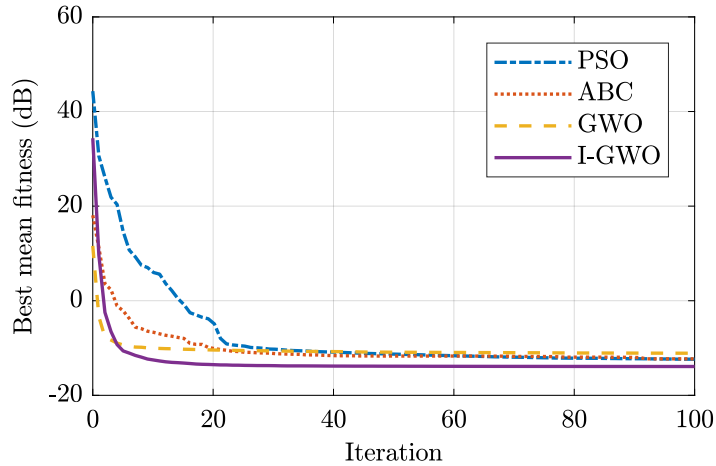


Figure 4: Average convergence curves for all algorithms considering a Monte Carlo experiment of 50 runs for example 1.

Algorithm	1-it. time (s)	It. to converge	Time to converge (s)
PSO	8.04	41	329.75
ABC	22.63	19	430.02
GWO	11.25	14	157.53
I-GWO	24.18	20	483.66

Table 2: Time for convergence of all algorithms for example 1.

Algorithm	median	$\sigma$	min	max
PSO	0.2032	0.2782	0.2017	2.1710
ABC	0.2334	0.0402	0.2025	0.4009
GWO	0.2489	0.0858	0.2017	0.4764
I-GWO	0.2017	$5.0516 \times 10^{-5}$	0.2017	0.2018

Table 3: Quantitative results from the box plot in terms of best fitness for example 1.

I-GWO obtained the most desired result in terms of  $\hat{M}_S$  considering the lack of outliers and a low dispersion. PSO had one outlier with  $\hat{M}_S > 2$ , whilst ABC obtained three outliers of higher  $\hat{M}_S$ , and the performance by the GWO algorithm for this problem was not satisfactory since there are too many solutions that achieved an  $\hat{M}_S$  higher than 2. Table 4 shows the quantitative data of the box plot presented in Figure 6, in agreement with what is commented over the results.

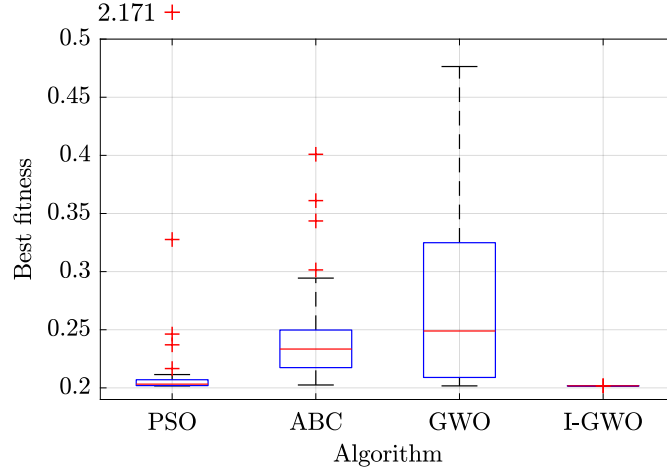


Figure 5: Box plot of a Monte Carlo experiment with 50 runs for all algorithms in terms of best fitness value obtained for example 1.

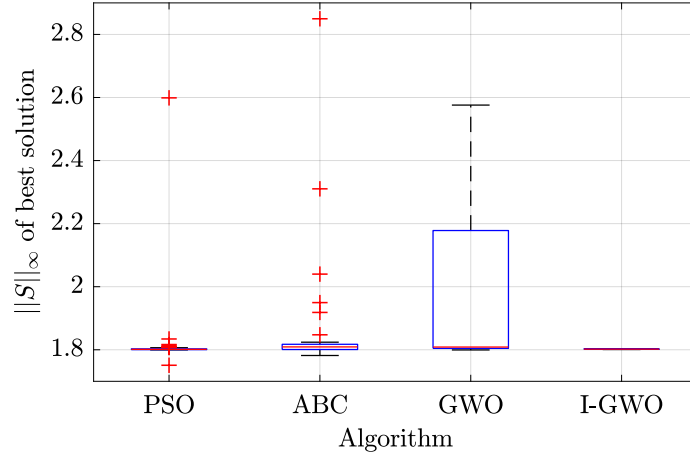


Figure 6: box plot of 50 runs for all algorithms in terms of  $\|S(z, \hat{\rho})\|_\infty$  value obtained for example 1.

### 7.2. Example 2: fourth-order plant

The fourth-order plant consists of

$$G_2(z) = \frac{0.1381(z - 0.95)(z^2 - 1.62z + 0.6586)}{(z^2 - 1.7z + 0.7325)(z^2 - 1.84z + 0.8564)}, \quad (36)$$

Algorithm	median	$\sigma$	min	max
PSO	1.8014	0.1130	1.7509	2.5988
ABC	1.8091	0.4740	$9.9798 \times 10^{-5}$	2.8496
GWO	1.8087	0.2923	1.7995	2.5760
I-GWO	1.8020	$4.5561 \times 10^{-4}$	1.8008	1.8030

Table 4: Quantitative results from the box plot in terms of  $\|S(z, \hat{\rho})\|_\infty$  for example 1.

with a time step of 1 second, which has the same structure as the model of a SEPIC converter [57]. Since the plant's zeros have minimum phase, which can be evaluated with data as aforementioned in Subsection 7.1, the VRFT method is used without flexible model reference criterion [23].

### 7.2.1. Data collection

For plant  $G_2(z)$ , the data is obtained the same way as described for example 1, in Subsection 7.1, with a PRBS signal of  $N = 2000$  samples applied to the closed-loop system with stabilizing controller,

$$k_p = \frac{0.5}{\|G_2(z)\|_\infty} = 0.3828, \quad (37)$$

considering additive white Gaussian noise with an SNR of 20 dB to represent measurement noise. The input-output set is formed by  $\{u, y\}_{k=1}^N$ .

### 7.2.2. Step 1 - VRFT

After the data is acquired, the next step is to use the VRFT to design a controller, which solves the cost function (8). For this example, the following control requirements are assumed: i) null steady-state error; ii) settling time of approximately 6.5 times faster than the closed-loop settling time with stabilizing controller  $k_p$ ; iii) null overshoot for a step reference. Considering such requirements, the choice of the reference model is done as suggested in [11], obtaining

$$Td(z) = \frac{1.4(z - 0.6)}{(z - 0.3)(z - 0.2)}. \quad (38)$$

Suppose a limited situation where only a PI controller is available, say for hardware limitations on a certain product. Therefore, the controller class to be considered is the PI class of controllers, resulting in

$$\bar{C}(z) = \left[ 1 \quad \frac{z}{z-1} \right]'. \quad (39)$$

The obtained VRFT solution for the problem results in the controller parameters

$$\hat{\rho} = [6.6568 \quad 3.3728], \quad (40)$$

which, via (3), results in the controller

$$C(z, \hat{\rho}) = \hat{\rho}' \bar{C}(z) = \frac{10.03(z - 0.6637)}{(z - 1)}. \quad (41)$$

Considering the VRFT-obtained solution (40), the robustness index of the system can be estimated according to Subsection 4, obtaining  $\hat{M}_S = 2.2767$ . As aforementioned, an  $M_S \leq 2$  is desired to ensure sufficient robustness [24], which leads to the application of the proposed solution.

### 7.2.3. Step 2 - Swarm intelligence algorithm

The swarm intelligence algorithms PSO, ABC, GWO, and I-GWO are applied to the problem (26) for the fourth-order plant case. The upper search bound is kept  $u_b = 10$  and lower bound  $l_b = 0$ , in order to increase the passivity of the controller as mentioned in Subsection 7.1. An upper bound of 10 should be sufficient, considering that the maximum desired robustness is not too far from the estimated robustness index at the end of step 1. The initial population spawn radius follows (28),  $R = (|u_b| + |l_b|)/2 = 5$ . A desired  $\|S(z, \hat{\rho})\|_\infty$  is set to 1.5, satisfying  $M_{Sd} \leq 2$ .

The number of agents of all algorithms is set to 50, with a maximum of 100 iterations per run. Each algorithm is run 50 times for different noise realizations, so that a proper analysis over the results can be made. For PSO and ABC algorithms, parameters are set as presented in Table 1. Aside from number of agents and maximum number of iterations, no other parameter is set by the user with the proposed GWO and I-GWO algorithm.

The average convergence curve of all algorithms for this case is presented in Figure 7. Table 5 presents the time for one iteration and how many iterations it took for the algorithms to converge. The hardware configuration is the same as in Example 1, as well as the convergence criteria  $\delta = 1 \times 10^{-3}$ . The ABC took a longer time to converge, followed by I-GWO, PSO, and at last, GWO. Figure 8 shows the box plot regarding best fitness value for each algorithms, for all runs. PSO, ABC, and I-GWO did not present far outliers, as those seen in the case of GWO. The quantitative values of the box plot are shown in Table 6, in agreement with the commented results.



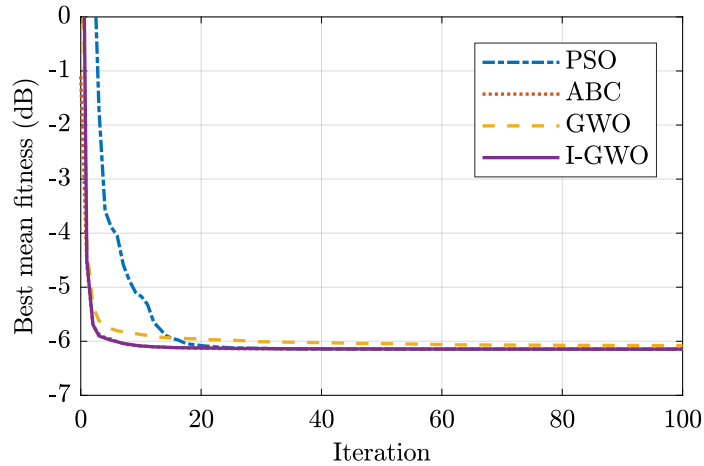


Figure 7: Average convergence curves for all algorithms considering a Monte Carlo experiment of 50 runs for example 2.

Alg.	1-it. time (s)	It. to converge	Time to converge (s)
PSO	7.24	20	144.72
ABC	22.93	10	229.32
GWO	7.55	9	68.00
I-GWO	22.34	9	201.10

Table 5: Time for convergence of all algorithms for example 2.

Algorithm	median	$\sigma$	min	max
PSO	0.49284	$2.2270 \times 10^{-9}$	0.49284	0.49284
ABC	0.49287	$4.7174 \times 10^{-5}$	0.49284	0.49303
GWO	0.49290	$1.0414 \times 10^{-2}$	0.49284	0.53568
I-GWO	0.49285	$6.4636 \times 10^{-6}$	0.49284	0.49286

Table 6: Quantitative results from the box plot in terms of best fitness for the example with system  $G_2(z)$ .

The  $\|S(z, \hat{\rho})\|_\infty$  norm obtained for the best solution at each run is shown in Figure 9, with its quantitative values presented in Table 7. Since all algorithms presented similar median, close enough to the desired  $M_S$  value, with considerably low dispersion, the algorithms that stand out are PSO and I-GWO, since they have the least number of outliers and the lower dispersion, which usually are desired results.

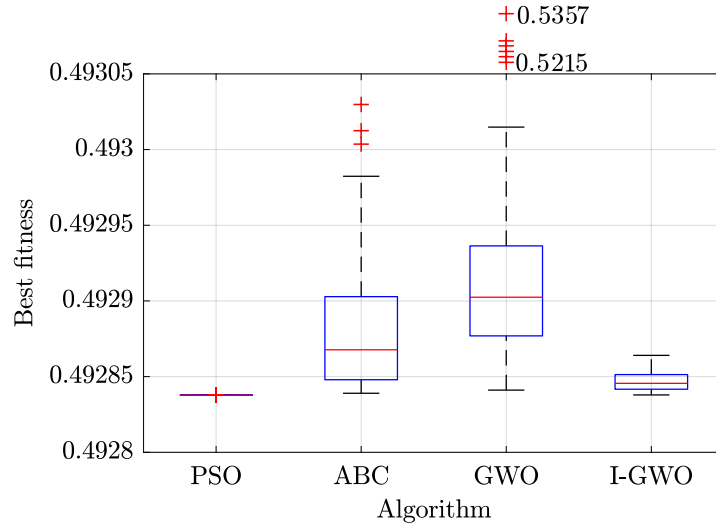


Figure 8: Box plot of a Monte Carlo experiment with 50 runs for all algorithms in terms of best fitness value obtained for example 2.

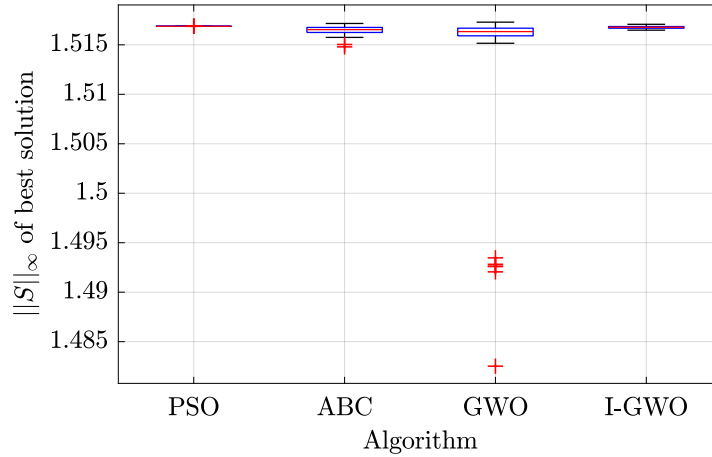


Figure 9: Box plot of a Monte Carlo experiment with 50 runs for all algorithms in terms of  $\|S(z, \hat{\rho})\|_\infty$  for example 2.

## 8. Conclusion

This work proposed a data-driven one-shot technique to increase the robustness of a closed-loop discrete-time system by changing the controller parameters using swarm intelligence algorithms. The considered optimiza-

Algorithm	median	$\sigma$	min	max
PSO	1.5169	$1.4558 \times 10^{-6}$	1.5169	1.5169
ABC	1.5165	$4.4060 \times 10^{-4}$	1.5148	1.5172
GWO	1.5133	$8.4447 \times 10^{-3}$	1.4825	1.5173
I-GWO	1.5168	$1.2216 \times 10^{-4}$	1.5165	1.5171

Table 7: Quantitative results from the box plot in terms of  $\|S(z, \hat{\rho})\|_\infty$  for example 2.

tion problem (26) is the VRFT cost function with a penalty regarding the value of the  $\|S(z, \rho)\|_\infty$  norm, which can be directly used as a measure of robustness. Such value is estimated via impulse response at each iteration of the metaheuristic algorithm.

Four swarm intelligence algorithms - PSO, ABC, GWO, and I-GWO - have been considered to illustrate the proposed technique with two real-world inspired plants. At both examples, the I-GWO obtained satisfactory results, presenting lower dispersion than other algorithms, less outliers, lower (best) fitness and acceptable values of  $\|S(z, \rho)\|_\infty$ . In the first example, although, PSO also achieved similar results to the I-GWO. The ABC and GWO algorithm performed worst in terms of dispersion, outliers and fitness. Additionally, I-GWO and ABC were the slowest algorithms to converge, and GWO the fastest.

As for future works, it is suggested: the inclusion of other constraints (e.g., for control effort) simultaneously with the robustness constraints; the use of other types of metaheuristics, as evolutionary or physics-based algorithms; the inclusion of a robustness constraint to the OCI, VDFT, or DD-LQR methods; extension of the current work for MIMO systems.

## 9. Acknowledgments

This study was financed in part by the Coordenação de Aperfeiçoamento de Pessoal de Nível Superior - Brasil (CAPES) - Finance Code 001, and partly by the Fundação de Amparo à Pesquisa e Inovação do Estado de Santa Catarina (FAPESC) - Grant number 288/2021.

## References

- [1] N. S. Nise, Control Systems Engineering, 3rd Edition, John Wiley & Sons, Inc., USA, 2000.

- [2] N. Chaudhuri, D. Chakraborty, B. Chaudhuri, Damping control in power systems under constrained communication bandwidth: A predictor corrector strategy, *IEEE Transactions on Control Systems Technology* 20 (1) (2012) 223–231, cited By 21. doi:10.1109/TCST.2010.2096817.
- [3] R. Xie, I. Kamwa, C. Y. Chung, A novel wide-area control strategy for damping of critical frequency oscillations via modulation of active power injections, *IEEE Transactions on Power Systems* 36 (1) (2021) 485–494. doi:10.1109/TPWRS.2020.3006438.
- [4] M. Kazimierczuk, *Pulse-width Modulated DC-DC Power Converters*, Wiley, 2008.  
URL [https://books.google.com.br/books?id=H\\_FwBkSpYY0C](https://books.google.com.br/books?id=H_FwBkSpYY0C)
- [5] T. Kobaku, S. C. Patwardhan, V. Agarwal, Experimental evaluation of internal model control scheme on a dc–dc boost converter exhibiting nonminimum phase behavior, *IEEE Transactions on Power Electronics* 32 (11) (2017) 8880–8891. doi:10.1109/TPEL.2017.2648888.
- [6] R. A. Aguiar, I. C. Franco, F. Leonardi, F. Lima, Fractional pid controller applied to a chemical plant with level and ph control, *Chemical Product and Process Modeling* 13 (2018).
- [7] V. Tharanidharan, R. Sakthivel, Y. Ren, S. Marshal Anthoni, Robust finite-time pid control for discrete-time large-scale interconnected uncertain system with discrete-delay, *Mathematics and Computers in Simulation* 192 (2022) 370–383. doi:10.1016/j.matcom.2021.08.024.
- [8] J. Tudon-Martinez, J.-J. Lozoya-Santos, A. Cantu-Perez, A. Cardenas-Romero, Advanced temperature control applied on an industrial box furnace, *Journal of Thermal Science and Engineering Applications* 14 (6), cited By 0 (2022). doi:10.1115/1.4052020.
- [9] N. van Tan, K. Dang, P. Dai, L. Van, Position control for haptic device based on discrete-time proportional integral derivative controller, *International Journal of Electrical and Computer Engineering* 12 (1) (2022) 269–276, cited By 0. doi:10.11591/ijece.v12i1.pp269-276.
- [10] L. H. Keel, S. P. Bhattacharyya, Controller synthesis free of analytical models: Three term controllers, *IEEE Transactions on Automatic Control* 53 (6) (2008) 1353–1369. doi:10.1109/TAC.2008.925810.

- [11] C. L. Remes, R. B. Gomes, J. V. Flores, F. B. Líbano, L. Campestrini, Virtual reference feedback tuning applied to dc–dc converters, *IEEE Transactions on Industrial Electronics* 68 (1) (2021) 544–552. doi:10.1109/TIE.2020.2967729.
- [12] I. Zenelis, X. Wang, A model-free sparse wide-area damping controller for inter-area oscillations, *International Journal of Electrical Power and Energy Systems* 136, cited By 0 (2022). doi:10.1016/j.ijepes.2021.107609.
- [13] H. Huang, X. Huang, W. Ding, M. Yang, D. Fan, J. Pang, Uncertainty optimization of pure electric vehicle interior tire/road noise comfort based on data-driven, *Mechanical Systems and Signal Processing* 165, cited By 0 (2022). doi:10.1016/j.ymsp.2021.108300.
- [14] H. Hjalmarsson, M. Gevers, S. Gunnarsson, O. Lequin, Iterative feedback tuning: theory and applications, *IEEE Control Systems Magazine* 18 (4) (1998) 26–41. doi:10.1109/37.710876.
- [15] A. Karimi, L. Mišković, D. Bonvin, Iterative correlation-based controller tuning, *International Journal of Adaptive Control and Signal Processing* 18 (8) (2004) 645–664. doi:https://doi.org/10.1002/acs.825.
- [16] M. Campi, A. Lecchini, S. Savaresi, Virtual reference feedback tuning: a direct method for the design of feedback controllers, *Automatica* 38 (8) (2002) 1337–1346. doi:https://doi.org/10.1016/S0005-1098(02)00032-8.  
URL <https://www.sciencedirect.com/science/article/pii/S0005109802000328>
- [17] L. C. Kammer, R. R. Bitmead, P. L. Bartlett, Direct iterative tuning via spectral analysis, *Automatica* 36 (9) (2000) 1301–1307. doi:https://doi.org/10.1016/S0005-1098(00)00040-6.
- [18] L. Campestrini, D. Eckhard, A. Sanfelice Bazanella, M. Gevers, Data-driven model reference control design by prediction error identification, *Journal of the Franklin Institute* 354 (6) (2017) 2628–2647, special issue on recent advances on control and diagnosis via process measurements. doi:https://doi.org/10.1016/j.jfranklin.2016.08.006.

- [19] D. Eckhard, L. Campestri, E. C. Boeira, Virtual disturbance feedback tuning, *IFAC Journal of Systems and Control* 3 (2018) 23–29, n/a. doi: <https://doi.org/10.1016/j.ifacsc.2018.01.003>.
- [20] G. R. GONÇALVES DA SILVA, A. S. Bazanella, C. Lorenzini, L. Campestri, Data-driven lqr control design, *IEEE Control Systems Letters* 3 (1) (2019) 180–185. doi:10.1109/LCSYS.2018.2868183.
- [21] J. A. R. Pérez, R. S. Llopis, Tuning and robustness analysis of event-based pid controllers under different event-generation strategies, *International Journal of Control* 91 (7) (2018) 1567–1587. doi:10.1080/00207179.2017.1322716.  
URL <https://doi.org/10.1080/00207179.2017.1322716>
- [22] S. Alcántara, R. Vilanova, C. Pedret, Pid control in terms of robustness/performance and servo/regulator trade-offs: A unifying approach to balanced autotuning, *Journal of Process Control* 23 (4) (2013) 527–542. doi:<https://doi.org/10.1016/j.jprocont.2013.01.003>.  
URL <https://www.sciencedirect.com/science/article/pii/S0959152413000139>
- [23] A. S. Bazanella, L. Campestri, D. Eckhard, *Data-Driven Controller Design: The H2 Approach*, Springer Publishing Company, Incorporated, 2014.
- [24] S. Skogestad, I. Postlethwaite, *Multivariable feedback control: Analysis and Design*, John Wiley, Hoboken, US-NJ, 2005.
- [25] S. Chiluka, S. Ambati, M. Seepana, U. Babu Gara, A novel robust virtual reference feedback tuning approach for minimum and non-minimum phase systems, *ISA Transactions* 115 (2021) 163–191. doi:10.1016/j.isatra.2021.01.018.
- [26] A. Karimi, C. Kammer, A data-driven approach to robust control of multivariable systems by convex optimization, *Automatica* 85 (2017) 227–233. doi:<https://doi.org/10.1016/j.automatica.2017.07.063>.
- [27] A. Nicoletti, M. Martino, A. Karimi, A robust data-driven controller design methodology with applications to particle accelerator power converters, *IEEE Transactions on Control Systems Technology* 27 (2) (2019) 814–821. doi:10.1109/TCST.2017.2783346.

- [28] J. Na, J. Zhao, G. Gao, Z. Li, Output-feedback robust control of uncertain systems via online data-driven learning, *IEEE Transactions on Neural Networks and Learning Systems* 32 (6) (2021) 2650–2662. doi:10.1109/TNNLS.2020.3007414.
- [29] J. Berberich, J. Köhler, M. A. Müller, F. Allgöwer, Data-driven model predictive control with stability and robustness guarantees, *IEEE Transactions on Automatic Control* 66 (4) (2021) 1702–1717. doi:10.1109/TAC.2020.3000182.
- [30] L. Campestri, D. Eckhard, M. Gevers, A. Bazanella, Virtual reference feedback tuning for non-minimum phase plants, *Automatica* 47 (8) (2011) 1778–1784. doi:https://doi.org/10.1016/j.automatica.2011.04.002.
- [31] D. G. Luenberger, Y. Ye, *Linear and Nonlinear Programming*, Springer Publishing Company, Incorporated, 2015.
- [32] D. Wolpert, W. Macready, No free lunch theorems for optimization, *IEEE Transactions on Evolutionary Computation* 1 (1) (1997) 67–82. doi:10.1109/4235.585893.
- [33] S. Mirjalili, *Genetic Algorithm*, Springer International Publishing, Cham, 2019.
- [34] B. Alatas, U. Can, Physics based metaheuristic optimization algorithms for global optimization, *American Journal of Information Science and Computer Engineering* (01 2015).
- [35] M. N. Ab Wahab, S. Nefti-Meziani, A. Atyabi, A comprehensive review of swarm optimization algorithms, *PLOS ONE* 10 (05 2015). doi:10.1371/journal.pone.0122827. URL https://doi.org/10.1371/journal.pone.0122827
- [36] S. Mirjalili, S. M. Mirjalili, A. Lewis, Grey wolf optimizer, *Advances in Engineering Software* 69 (2014) 46–61. doi:https://doi.org/10.1016/j.advengsoft.2013.12.007.
- [37] J. Kennedy, R. Eberhart, Particle swarm optimization, in: *Proceedings of ICNN'95 - International Conference on Neural Networks*, Vol. 4, 1995, pp. 1942–1948 vol.4. doi:10.1109/ICNN.1995.488968.

- [38] D. Karaboga, An idea based on honey bee swarm for numerical optimization, Tech. rep., Erciyes University, Engineering Faculty (2005).
- [39] M. H. Nadimi-Shahraki, S. Taghian, S. Mirjalili, An improved grey wolf optimizer for solving engineering problems, *Expert Systems with Applications* 166 (2021) 113917. doi:<https://doi.org/10.1016/j.eswa.2020.113917>.
- [40] G. C. Goodwin, S. F. Graebe, M. E. Salgado, *Control System Design*, 1st Edition, Prentice Hall PTR, USA, 2000.
- [41] L. Ljung, *System Identification (2nd Ed.): Theory for the User*, Prentice Hall PTR, USA, 1999.
- [42] L. V. Fiorio, Virtual reference feedback tuning with robustness constraints: a swarm intelligence solution, Master’s thesis, Universidade do Estado de Santa Catarina (2022). doi:[10.13140/RG.2.2.19418.41927](https://doi.org/10.13140/RG.2.2.19418.41927).
- [43] G. R. Gonçalves da Silva, A. S. Bazanella, L. Campestrini, One-shot data-driven controller certification, *ISA transactions* 99 (2020) 361—373. doi:[10.1016/j.isatra.2019.10.011](https://doi.org/10.1016/j.isatra.2019.10.011).
- [44] T. Chen, H. Ohlsson, L. Ljung, On the estimation of transfer functions, regularizations and gaussian processes—revisited, *Automatica* 48 (8) (2012) 1525–1535. doi:<https://doi.org/10.1016/j.automatica.2012.05.026>.
- [45] S. L. Brunton, J. N. Kutz, *Data-Driven Science and Engineering: Machine Learning, Dynamical Systems, and Control*, 1st Edition, Cambridge University Press, USA, 2019.
- [46] T. Chen, L. Ljung, Implementation of algorithms for tuning parameters in regularized least squares problems in system identification, *Automatica* 49 (7) (2013) 2213–2220. doi:<https://doi.org/10.1016/j.automatica.2013.03.030>.
- [47] The MathWorks Inc., Natick, Massachusetts, United States, *System Identification Toolbox Release 2017b* (2021).
- [48] L. V. Fiorio, C. L. Remes, Y. R. de Novaes, *impulseest*: A python package for non-parametric impulse response estimation with input–output



- data, SoftwareX 15 (2021) 100761. doi:<https://doi.org/10.1016/j.softx.2021.100761>.
- [49] S. Yerramilli, A. Tangirala, `sysid`: system identification in R, R Foundation for Statistical Computing (2017).
- [50] K.-L. Du, M. N. S. Swamy, Search and Optimization by Metaheuristics: Techniques and Algorithms Inspired by Nature, 1st Edition, Birkhäuser Basel, 2016.
- [51] E. Bonabeau, M. Dorigo, G. Theraulaz, Swarm Intelligence: From Natural to Artificial Systems, Oxford University Press, Santa Fe Institute Studies in the Sciences of Complexity, 2001.
- [52] D. Karaboga, B. Basturk, Artificial bee colony (abc) optimization algorithm for solving constrained optimization problems, in: P. Melin, O. Castillo, L. T. Aguilar, J. Kacprzyk, W. Pedrycz (Eds.), Foundations of Fuzzy Logic and Soft Computing, Springer Berlin Heidelberg, Berlin, Heidelberg, 2007, pp. 789–798.
- [53] E.-G. Talbi, Metaheuristics: From Design to Implementation, Vol. 74, John Wiley, 2009. doi:[10.1002/9780470496916](https://doi.org/10.1002/9780470496916).
- [54] R. W. Erickson, D. Maksimovic, Fundamentals of Power Electronics, 2nd Edition, Springer, 2001.
- [55] J. Bao, L. Peter, Process Control: The Passive Systems Approach, Springer Publishing Company, Incorporated, 2007. doi:[10.1007/978-1-84628-893-7](https://doi.org/10.1007/978-1-84628-893-7).
- [56] M. K. Heris, The Yarpiz Project (2015).  
URL <https://yarpiz.com/about>
- [57] E. V. Kassick, Deriving the canonical equivalent circuit for small signal & low frequency ac model for the sepic and zeta pwm dc-dc converters with two-port network (quadripoles) circuit analysis technique, Eletr. Potên. 16 (2011) 376–382. doi:<http://dx.doi.org/10.18618/REP.20114.376382>.